

# Three-Dimensional Graphene Supported Nickel Molybdate Nanowires as Novel Ultralight and Flexible Electrode for Supercapacitors

Xiaozhi Liu<sup>a,†</sup>, Ke Zhang<sup>a,†</sup>, Baolin Yang<sup>b</sup>, Wenlei Song<sup>b</sup>, Qian Liu<sup>b</sup>, Fei Jia<sup>a</sup>, Shiyi Qin<sup>a</sup>,  
Wanjuan Chen<sup>b</sup>, Jian Li<sup>b,c,\*</sup>, Zhenxing Zhang<sup>b,c,\*</sup>

<sup>a</sup> Cuiying Honors College, Lanzhou University, Lanzhou 730000, P. R. China

<sup>b</sup> School of Physical Science and Technology, Lanzhou University, Lanzhou 730000, P.  
R. China

<sup>c</sup> Key Laboratory for Magnetism and Magnetic Materials of the Ministry of Education,  
Lanzhou University, Lanzhou 730000, P. R. China

<sup>†</sup> These authors contributed equally to this work.

\* Corresponding author. Tel.: +86 931 8912753; fax: +86 931 8913554.  
E-mail addresses: zhangzx@lzu.edu.cn (Z. Zhang), jianli@lzu.edu.cn (J. Li).

**ABSTRACT:** Graphene/ nickel molybdate (NiMoO<sub>4</sub>) nanowires composite networks as positive electrode materials for supercapacitors were fabricated via a facile hydrothermal method. The X-ray diffraction and Raman results show that NiMoO<sub>4</sub> is  $\alpha$  phase. The high specific capacitance of 2630.4 F g<sup>-1</sup> at a current density of 12 A g<sup>-1</sup> and the good reversibility with a cycling efficiency of 97.3% after 1000 cycles were obtained by the electrochemical measurements. Furthermore, the energy density reaches 365.33 Wh kg<sup>-1</sup> at a steady power density of 11618.27 W kg<sup>-1</sup>. These inspiring performances demonstrate the potential of the designed electrodes for the future flexible and lightweight energy storage systems.

**KEYWORDS:** GRAPHENE; NICKEL MOLYBDATE; HYDROTHERMAL METHOD; SUPERCAPACITOR.

## 1. INTRODUCTION

Supercapacitors are an alternative environmentally friendly energy storage system to combine the advantages of primary/secondary batteries and conventional physical capacitors in terms of high power and high energy density, long lifespan, wide range of working temperature and rapid recharging rate. <sup>[1]</sup> In particular, flexible and ultralight supercapacitors have become one of the most intense research areas, not only due to their potential applications in portable electronic devices, such as wearable mobile phones and foldable electronic papers, <sup>[2]</sup> but also due to their promising applications in hybrid power systems of high energy efficiency, such as hybrid electric vehicle and astronautic energy supply. <sup>[3]</sup>

As a novel supercapacitors' backbone material, the flexible three-dimensional (3D) graphene of high specific surface area ( $392 \text{ m}^2 \text{ g}^{-1}$ ) and high electrical conductivity ( $55 \text{ S cm}^{-1}$ ), is a self-supporting and binder-free electrode material with low mass density of about  $0.75 \text{ mg cm}^{-2}$  and low specific capacitance of about  $5.57 \times 10^{-5} \text{ F cm}^{-2}$  <sup>[4]</sup>. Besides transition metal oxides like  $\text{MnO}_2$  <sup>[5]</sup>,  $\text{Co}_3\text{O}_4$  <sup>[6]</sup>,  $\text{NiO}$  <sup>[7]</sup>,  $\text{RuO}_2$  <sup>[8]</sup>, the binary metal oxides with multiple oxidation states have also been considered as promising pseudocapacitor electrode materials because they enable rich redox reactions and high specific capacitances. Among them,  $\text{NiMoO}_4$  has drawn great research attention because of its higher electrical conductivity, low cost, chemical and thermal stability,

abundance and environment benignity. Recently, the nanoparticles <sup>[9]</sup>, nanorods <sup>[10]</sup>, nanoclusters <sup>[11]</sup>, nanospheres <sup>[12]</sup> and nanosheets <sup>[13]</sup> of NiMoO<sub>4</sub> for supercapacitors have been reported, and their largest specific capacitance reaches to 1517 F g<sup>-1</sup> <sup>[9]</sup>. However, due to the lack of good current collectors, their potential electrochemical performance was inhibited seriously. Di Guo *et al.* reported NiMoO<sub>4</sub> nanowires supported on Ni foam which exhibit a high specific capacitance of 2083 F g<sup>-1</sup> at a current density of 8 mA cm<sup>-2</sup> owing to the one-dimensional array structure and the high conductance of the current collector. <sup>[14]</sup> Although it reaches a higher specific capacitance, the Ni foam (around 37 mg cm<sup>-2</sup>) used here is too heavy for supercapacitors to be applied widely. Therefore, how to find a suitable current collector to improve NiMoO<sub>4</sub> electrodes' efficient energy storage at high recharging rates and fully realize the advantage of the active materials remains a central challenge.

Herein, we firstly fabricated NiMoO<sub>4</sub> nanowires strongly anchored on 3D graphene networks by a simple one-pot hydrothermal synthesis coupled with a calcination treatment. The as-prepared flexible bulk electrodes permit electron to transfer uninterruptedly through robust interconnected graphene skeleton, and electrolyte ions to diffuse and form electroactive double-layer reaction sites easily due to spongy structure and large accessible surface area, which contribute to a high area specific capacitance of 1.99 F cm<sup>-2</sup> (1987.2 F g<sup>-1</sup>) at 54 A g<sup>-1</sup> and a good cycling stability of 97.3% (1933.2 F g<sup>-1</sup>) after 1000 cycles. Besides, at a current density of 12 A g<sup>-1</sup>, the specific capacitance even reaches to 2630.4 F g<sup>-1</sup> which is higher than the reported results. <sup>[9-15]</sup> Furthermore, considering the total mass of this electrode is only 1.75 mg,

the specific capacitance of the entire electrode still reaches to  $1503.1 \text{ F g}^{-1}$  at  $12 \text{ A g}^{-1}$ , which is much higher than the reported  $\text{NiMoO}_4/\text{Ni}$  foam electrode ( $54.1 \text{ F g}^{-1}$  at  $8 \text{ mA cm}^{-2}$  as carefully calculated).<sup>[14]</sup> These results reveal that the 3D graphene/ $\text{NiMoO}_4$  nanowires composite is a promising electrode materials in the development and practical applications of high-performance flexible supercapacitors.

## 2. EXPERIMENTS AND METHODS

### 2.1. Growth of the 3D Graphene Networks

Nickel foams (Changsha Lyrun New Material Co. Ltd., China), were used as templates for the chemical vapor deposition (CVD) growth of graphene. After cut into pieces and placed in a quartz tube, they were then heated to  $1000 \text{ }^\circ\text{C}$  under Ar ( $200$  standard cubic centimeters per minute (sccm)) and  $\text{H}_2$  ( $50$  sccm) and annealed for  $10$  min to eliminate a thin surface oxide layer, followed by introducing a small amount of  $\text{CH}_4$  ( $2.5$  sccm) at ambient pressure. After  $10$ -min flow of reaction gas mixture, the sample were rapidly cooled to room temperature, then taken out and immersed into  $6 \text{ M HCl}$  solution at  $80 \text{ }^\circ\text{C}$  for  $3.5 \text{ h}$  to completely dissolve the Ni foam to obtain the 3D graphene.

### 2.2. Preparation of 3D graphene/ $\text{NiMoO}_4$ composite

In a typical synthesis of 3D graphene/ $\text{NiMoO}_4$  composite,  $1.5 \text{ mmol}$  of  $\text{Ni}(\text{NO}_3)_2 \cdot 6\text{H}_2\text{O}$  and  $1.5 \text{ mmol}$  of  $\text{Na}_2\text{MoO}_4 \cdot 7\text{H}_2\text{O}$  are added in  $30 \text{ mL}$  deionized water and then shifted into Teflon-lined autoclave liner at room temperature. The 3D graphene was infiltrated by one drop of ethanol in advance and then immersed into the reaction

solution in the liner, which was then sealed in stainless steel autoclave and kept at 150 °C for 6 h and then cooled down to 30 °C naturally. The uniformly coated composite was taken out and washed by ultra-sonication in distilled water and subsequently acetone for a few seconds, then dried in a drying box at 80 °C for 12 h. Finally, the 3D graphene with the as-prepared hydrate precursors was annealed at 300 °C for 1 h in pure Ar to obtain NiMoO<sub>4</sub> networks.

### *2.3. Electrochemical performance measurement*

In half cell tests, a three-electrode system was employed and a 2 M KOH aqueous solution was used as electrolyte where the 3D graphene/NiMoO<sub>4</sub> composite was used as working electrode, a standard calomel electrode (SCE) as reference electrode, and Pt plate as counter electrode. All the measurements were carried out at room temperature using an electrochemical workstation (RST5200, Zhengzhou Shiruisi Instrument Technology Co., Ltd., China).

### *2.4. Material Characterization*

The morphologies of the samples were characterized by field emission scanning electron microscopy (FE-SEM, Hitachi S-4800), with an accelerating voltage of 5 kV. Grazing-angle X-ray diffraction (XRD, Philips, X'pert pro, Cu Ka, 0.154056 nm) was employed to characterize the crystal structure of the samples. The mass of NiMoO<sub>4</sub> nanomaterials was measured by a microbalance (Mettler, XS105DU) with the tolerance of less than 0.01 mg.

## **3. RESULTS AND DISCUSSION**

### 3.1. Microstructure characterizations

Figure 1a and 1b show the SEM images of Graphene/NiMoO<sub>4</sub> nanowires networks with low- and high-resolution respectively. The mass loading is 1.05 mg cm<sup>-2</sup> and the length of NiMoO<sub>4</sub> nanowires is about 5 μm with a diameter of around 120 nm, which were uniformly anchored on the 3D Graphene networks. However, some cracks can be observed in figure 1a because the ethanol couldn't soak the graphene very well before hydrothermal process.

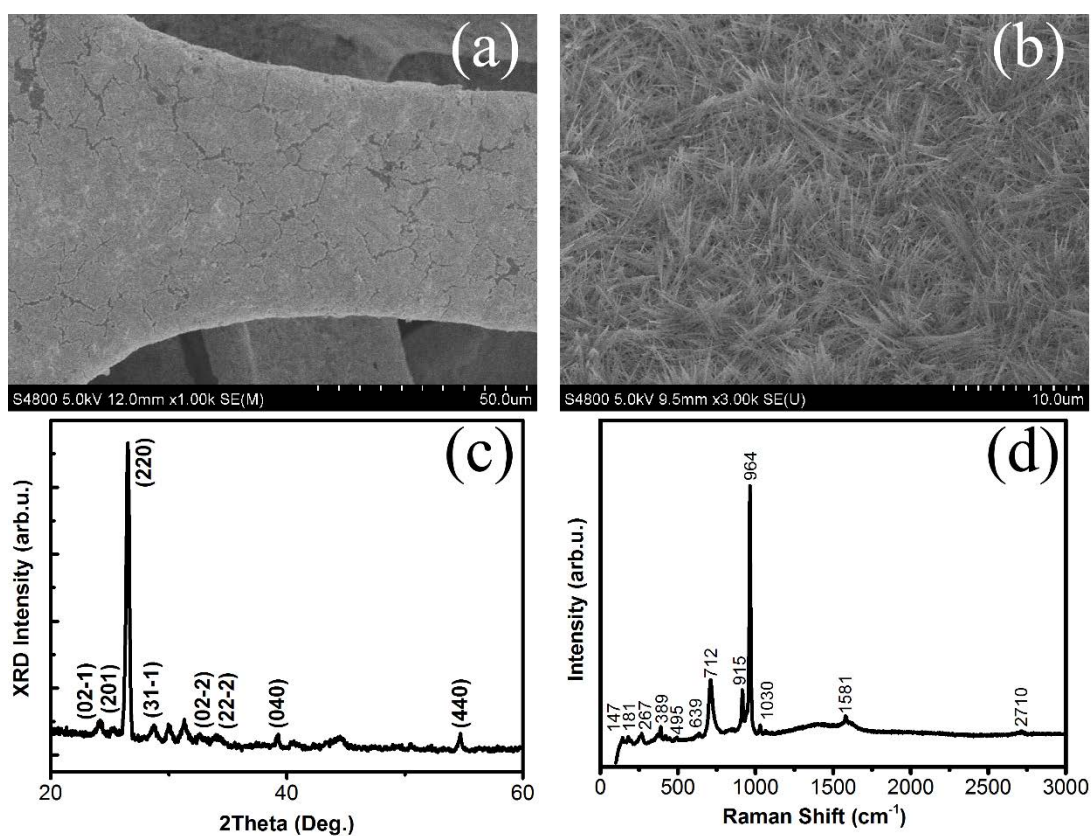


Figure 1 SEM image of Graphene/NiMoO<sub>4</sub> nanowires networks (a) and NiMoO<sub>4</sub> nanowires (b), XRD pattern of the Graphene/NiMoO<sub>4</sub> networks (c), and Raman spectra of the Graphene networks and Graphene/NiMoO<sub>4</sub> networks (d).

The crystallinity of the electrodeposited NiMoO<sub>4</sub> nanowires was determined by

Raman spectroscopy and XRD, as shown in Fig. 1c and 1d respectively. The labeled diffraction peaks in Fig. 1c correspond to  $\alpha$ -NiMoO<sub>4</sub> phase from JCPDF card (No. 45-0142) and other peaks are from graphite phase. As shown in Fig. 1d, except for the characteristic G and 2D peaks from graphene skeleton, the peaks from 100 to 1500 cm<sup>-1</sup> are from  $\alpha$ -NiMoO<sub>4</sub>, and amongst them, the three strong peaks 964, 915 and 712 cm<sup>-1</sup> are its characteristic peaks. [16] The result from Raman spectra is highly consistent with the XRD patterns and there are no other peaks appeared, which demonstrated that the Graphene/NiMoO<sub>4</sub> nanowires networks are of high degree of purity and crystallinity.

### 3.2. Electrochemical performances

Fig. 2a shows the cyclic voltammograms (CVs) of the 3D graphene/NiMoO<sub>4</sub> electrode at various scan rates as the potential ranging from -0.2 to 0.8 V. The cyclic voltammetry (CV) curves are nearly symmetrical and display a pair of strong redox peaks indicating that the capacitive characteristics are mainly dominated by Faradaic reaction and the contribution from the electrical double-layer capacitance is negligible. At a low scan rate of 5 mV s<sup>-1</sup>, the anodic peak at 0.34 V is credited to the oxidation process, and the cathodic peak at 0.17 V owes to the reduction process. [14] As the scan rates become higher, the anodic and the cathodic peaks move to higher and lower potentials respectively, suggesting it is a quasi reversible process. Furthermore, the responding peak current increases almost linearly with the increasing scan rates, which implies the diffusion of OH<sup>-</sup> ions between the electrolyte and the electrode is uninterrupted and fast enough to keep pace with the scanning rate.

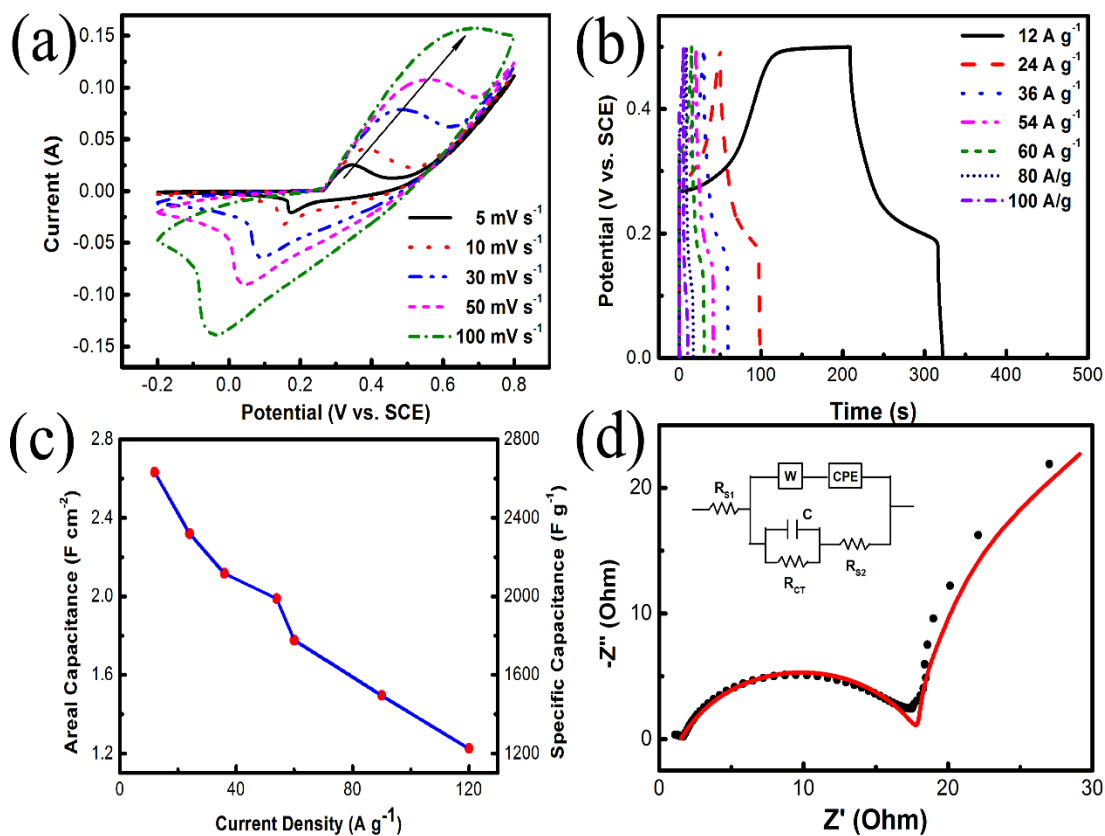


Figure 2 CVs of Graphene/NiMoO<sub>4</sub> nanowires networks at different scan rate (a), GCDs of Graphene/NiMoO<sub>4</sub> networks at different current density (b), Areal and Specific Capacitance vs. current density for Graphene/NiMoO<sub>4</sub> networks (c), EIS plot of Graphene/NiMoO<sub>4</sub> networks from 0.001 Hz to 100 kHz at 50 mV (d).

Galvanostatic charge-discharge (GCD) curves in Fig. 2b conducted in the potential range between 0 and 0.5 V reveal a pair of plateau regions corresponding to the peaks in the CVs. At a small current density of 12 A g<sup>-1</sup>, the anodic and cathodic plateau regions are respectively around 0.28 V and 0.22 V, which separate from each other farther as the current density gets larger. Impressively, the composite electrode delivers high specific capacitance of 2630.4, 2318.4, 2116.8, 1987.2, 1776.0, 1494.0, and 1224.0 F g<sup>-1</sup> at discharge current densities of 12, 24, 36, 54, 60, 90 and 120 A g<sup>-1</sup> respectively

as shown in Fig. 2c, which demonstrates the 3D graphene/NiMoO<sub>4</sub> electrode possesses a high rate capability. The power density (P, kW kg<sup>-1</sup>) and energy density (E, Wh kg<sup>-1</sup>) from the charge/discharge curves can be deduced based on equations <sup>[17]</sup> :

$$\begin{aligned} E &= 0.5 \cdot C \cdot (\Delta V)^2 \\ P &= E/t \end{aligned} \quad (1)$$

At the current densities of 12 A g<sup>-1</sup>, the resulting energy density is 365.33 Wh kg<sup>-1</sup> and the power density reaches 11618.27 W kg<sup>-1</sup>, which is higher than the NiMoO<sub>4</sub> nanorods/graphene (4.53 Wh kg<sup>-1</sup> and 1125 W kg<sup>-1</sup> at 5 A g<sup>-1</sup>). <sup>[15]</sup>

For a further investigation of the designed 3D composite structure, the electrochemical impedance spectroscopy (EIS) measurement was carried out in frequencies ranging from 0.001 Hz to 100 kHz at open circuit voltage with an AC voltage perturbation amplitude of 50 mV (Fig. 2d). In the high-frequency region of the Nyquist plot, the characteristic impedance semicircle is mainly governed by the charge transferring process and related to the relaxation time. Whereas, the tilting line in the low frequency zone is the feature of the electrolyte ions diffusion controlled faster kinetic process. <sup>[15]</sup> The simultaneous appearance of them is related to the speed difference of the electrolyte and charge transferring process, which further confirms the electrode is a quasi reversible system. Meanwhile, the deviation of the high frequency arc from standard semicircle and the low frequency arc from straight line are mainly caused by the high porosity of our three-dimensional system, for which the conventional two-dimensional plate approximation is no longer suitable. The EIS data have been fitted with an equivalent electrical circuit (as shown in the inset of Fig. 2d) with a minimized chi-squared ( $\chi^2$ ) value in the order of 10<sup>-3</sup>, which consists of R<sub>S1</sub> the

intrinsic resistance of composite electrode,  $R_{CT}$  the charge transfer resistance caused by the faradaic reactions of  $NiMoO_4$  between different oxidation states,  $R_{S2}$  the ionic resistance of electrolyte, CPE the constant phase element, W the Warburg type diffusion element and C the pseudo-capacitance from  $NiMoO_4$  nanowires with very little double layer capacitance. The intersecting point of the semicircle with the real axis gives the  $RS1$  1.59 Ohm which is consistent with the simulation result 1.49 Ohm, and the simulated specific capacitance  $2.31 \text{ F cm}^{-2}$  is also consistent with the GCD measurements.

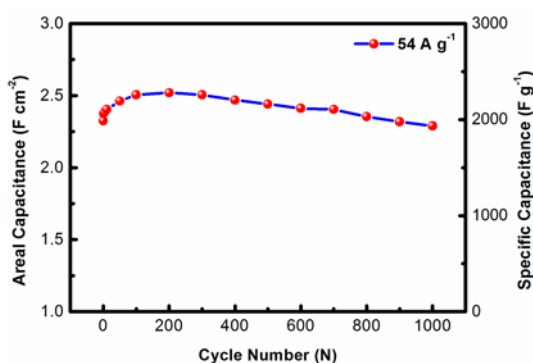


Figure 3 Cycling performance of Graphene/ $NiMoO_4$  nanowires networks for charging and discharging at a current density of  $54 \text{ mA cm}^{-2}$ .

The electrochemical cycle stability test was performed at a mild current density of  $54 \text{ mA cm}^{-2}$  in the range of 0-0.5 V in the same alkaline electrolyte, as shown in Fig. 3. The initial specific capacitance for the first cycle is  $1987.2 \text{ F g}^{-1}$  which then rapidly rises to  $2106 \text{ F g}^{-1}$  at the first tenth cycle and achieves the maximum value of  $2278.8 \text{ F g}^{-1}$  at the two hundredth cycle. The reason for this initial improvement is that the Graphene/ $NiMoO_4$  electrode was gradually soaked and the electrolyte ions were transported to deeper inside the networks. Then the electrode's specific capacitance

drops slowly to  $1933.2 \text{ F g}^{-1}$  after another 800 cycles' testing due to the dissolution of some  $\text{NiMoO}_4$  during the charge/discharge cycling, which displays a long-term cycle stability of the 3D graphene/ $\text{NiMoO}_4$  composite electrode under large current density and indicates its underlying qualification for future practical applications.

#### **4. CONCLUSIONS**

In summary, we have successfully constructed  $\text{NiMoO}_4$  nanowires on 3D graphene with outstanding pseudocapacitive performance for supercapacitors, using a scalable and self-assembly strategy. The as-prepared electrodes provide an excellent cyclic stability and a high value of specific capacitance about  $1224.0 \text{ F g}^{-1}$  even at a very high current density of  $120 \text{ A g}^{-1}$ . These 3D graphene supported composites exhibit flexibility, fine durability, lightweight quality and even ultrahigh specific capacitance of  $1503.1 \text{ F g}^{-1}$  at  $12 \text{ A g}^{-1}$  with respect to the total mass of the electrode. Our work confirms the 3D graphene is a class of superior current collector for the future flexible supercapacitors, and illuminates a new way to utilize the capacitive performance of the electroactive materials.

#### **ACKNOWLEDGMENTS**

This research was supported by the National Natural Science Foundation of China (Nos.: 51302122, 51202100), the Natural Science Foundation of Gansu Province in China (No: 1208RJZA227), and the National Training Program of Innovation Entrepreneurship for Undergraduates of Lanzhou University (No. 860605).

## REFERENCES

- [1] J. R. Miller and P. Simon, *Science* **321**, 651 (2008).
- [2] J. A. Rogers and Y. Huang, *Proc. Natl. Acad. Sci. U.S.A.* **106**, 10875 (2009).
- [3] H. Nishide and K. Oyaizu, *Science* **319**, 737 (2008).
- [4] Y. He, W. Chen, X. Li, Z. Zhang, J. Fu, C. Zhao, and E. Xie, *ACS Nano* **7**, 174 (2013).
- [5] M. Huang, Y. Zhang, F. Li, L. Zhang, R. S. Ruoff, Z. Wen, and Q. Liu, *Sci. Rep.* **4**, 3878 (2014).
- [6] C. Xiang, M. Li, M. Zhi, A. Manivannan, and N. Wu, *J. Power Sources* **226**, 65 (2013).
- [7] M. Yu, W. Wang, C. Li, T. Zhai, X. Lu, and Y. Tong, *NPG Asia Mater.* **6**, e129 (2014).
- [8] Z.-S. Wu, D.-W. Wang, W. Ren, J. Zhao, G. Zhou, F. Li, and H.-M. Cheng, *Adv. Funct. Mater.* **20**, 3595 (2010).
- [9] B. Senthilkumar, K. Vijaya Sankar, R. Kalai Selvan, M. Danielle, and M. Manickam, *RSC Adv.* **3**, 352 (2013).
- [10] M.-C. Liu, L. Kang, L.-B. Kong, C. Lu, X.-J. Ma, X.-M. Li, and Y.-C. Luo, *RSC Adv.* **3**, 6472 (2013).
- [11] H. Wan, J. Jiang, X. Ji, L. Miao, L. Zhang, K. Xu, H. Chen, and Y. Ruan, *Mater. Lett.* **108**, 164 (2013).
- [12] D. Cai, D. Wang, B. Liu, Y. Wang, Y. Liu, L. Wang, H. Li, H. Huang, Q. Li, and

- T. Wang, *ACS Appl. Mater. Interfaces* **5**, 12905 (2013).
- [13] D. Cai, B. Liu, D. Wang, Y. Liu, L. Wang, H. Li, Y. Wang, C. Wang, Q. Li, and T. Wang, *Electrochim. Acta* **115**, 358 (2014).
- [14] D. Guo, P. Zhang, H. Zhang, X. Yu, J. Zhu, Q. Li, and T. Wang, *J. Mater. Chem. A* **1**, 9024 (2013).
- [15] D. Ghosh, S. Giri, and C. K. Das, *Nanoscale* **5**, 10428 (2013).
- [16] J. Haetge, I. Djerdj, and T. Brezesinski, *Chem. Commun.* **48**, 6726 (2012).
- [17] Y. He, W. Chen, J. Zhou, X. Li, P. Tang, Z. Zhang, J. Fu, and E. Xie, *ACS Appl. Mater. Interfaces* **6**, 210 (2013).